A mixed-valence $(Fe^{II})_2(Fe^{III})_2$ square for molecular expression of quantum cellular automata†

Yonggang Zhao, Dong Guo, Yang Liu, Cheng He and Chunying Duan*

Received (in Cambridge, UK) 30th June 2008, Accepted 4th September 2008
First published as an Advance Article on the web 30th September 2008
DOI: 10.1039/b811061a

A di-mixed-valence molecular square $(Fe^{II})_2(Fe^{III})_2$ with two extra mobile electrons (or holes) occupying the opposite corners is achieved *via* self-assembly as a pure phase with remarkable stability for molecular expression of quantum cellular automata (QCA).

The synthetic accessibility by self-assembly of two-dimensional switchable arrays of nanometric size complements theoretical developments in molecular information storage and processing.[1] The gridlike metal ion arrays, which incorporate a set of metal ions in a regular network of organic ligands, have been underlined as promising components in molecular-based electronics technology, because of their physicochemically addressable and switchable properties.[2] Especial interests in these architectures might arise from an alternative encoding concept called "cellular automata", in which binary information encoded in the charge configuration of a cell composed of a small number of differently charged redox centers is transmitted *via* coupled electric fields rather than electron currents.[3,4] Envisaged first for quantum dots, the binary states are represented by the location of two mobile electrons at opposite corners of the square due to Coulombic repulsion. For practical operation, molecule-sized QCA cells are required to generate energy differences between state configurations that are larger than the thermal energy, k_BT, at room temperature[5,6] in the presence of an applied electric field. In this case, a molecular square having di-mixed-valence states with a D_{4h} symmetry would be a versatile candidate for a four-dots molecular QCA cell.

Though the rational assemblies of metal complexes open the door for exploring the well-isolated and characterized molecular squares[7,8] with di-mixed-valence states, the construction of mixed-valence molecular squares exhibiting promising electrochemical behaviors, thermodynamic stability associated with charge disproportionation and kinetic stability relative to degradation reactions still remain substantial challenges. To address this problem, we build a molecular square by using thiocarbohydrazones as initial units owing to the inherent conformational restraints of the chelating motif and the role of bridging atoms/groups in each side of squares, which would favor the stability of the squares.[9] Additionally, the negative charges of these anionic chelators that originate from metal-induced deprotonation would lead the whole molecule to be a relatively lower charged species. This special structural fashion would be beneficial to modulating the electron distribution in the square[9] and diminishing the need for counterions.

Reaction of the ligand H_2L (bis[phenyl(2-pyridyl)methanone] thiocarbohydrazone) with $FeSO_4{\cdot}7H_2O$ in the presence of $NaClO_4$ gave a new compound $Fe_4L_4(ClO_4)_2{\cdot}H_2O$ [**1**$(ClO_4)_2{\cdot}H_2O$]. The ESI-MS spectrum (see supporting information,† Fig. S1) of the compound exhibits only one intense peak at m/z 980.63 with isotopic distribution patterns separated by 0.5 ± 0.05 Da, which is assigned to the mixed-valence species $[Fe^{II}{}_2Fe^{III}{}_2(L)_4]^{2+}$. This result clearly shows the pronounced thermodynamic stability of the mixed-valence tetranuclear fragment in solution without disassembling. X-Ray crystallographic data unequivocally confirms the existence of a di-mixed-valence tetranuclear cationic molecular square of $\mathbf{1}^{2+}$.‡

As shown in Fig. 1, the cation is composed of four iron ions and four deprotonated ligands L^{2-} with each iron atom being positioned at each corner of the square. There are two ligands bonding to each iron in *mer* configuration, where the pairs of sulfur atoms and pyridine nitrogen atoms bear a *cis*-relationship, respectively, while the thiocarbohydrazone nitrogen atoms are *trans* to each other. Each sulfur atom lies at the mid-point of each edge of the square and bridges two metal atoms with the M···M separation being about 4.2 Å. The C–N and N–N bond distances of the thiocarbohydrazone moieties are intermediate between formal single and double bonds,

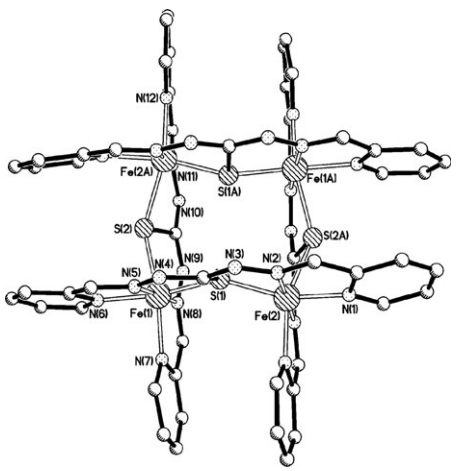

Fig. 1 Molecular structure of the cationic square $\mathbf{1}^{2+}$. Hydrogen atoms, the phenyl rings and one pair of the disordered sulfur atoms are omitted for clarity. Selected interatomic separations (Å): Fe–S 2.19(4), Fe–N_{imine} 1.93(1), Fe–N_{nu} 1.96(1), C–S 1.81(2), N–N 1.36(1), C–N_{imine} 1.31(2), Fe(1)···Fe(2) 4.16(1) (av.). Symmetry code A: $-x, y, -z + 1/2$.

State Key Laboratory of Fine Chemicals, Dalian University of Technology, Dalian, 116012, China. E-mail: cyduan@dlut.edu.cn

† Electronic supplementary information (ESI) available: Experimental details, ESI-MS spectra, magnetic susceptibility data and UV-Vis spectra. Crystal data for compound **1**$(ClO_4)_2{\cdot}H_2O$. CCDC 650544. For ESI and crystallographic data in CIF or other electronic format see DOI: 10.1039/b811061a

reflecting the extensively delocalized nature of the ligand moiety over the entire molecular skeleton. The short metal···metal separations and the extensive electron delocalization of the ligand skeleton would substantially enhance the electronic communication between the metal centers and thus significantly stabilize the mixed-valence species, which could provide a good opportunity to isolate the mixed-valence complex in a pure phase without being labile with respect to charge disproportionation.[10]

The redox properties of $\mathbf{1}(ClO_4)_2{\cdot}H_2O$ were investigated by means of cyclic voltammetry (CV) and differential pulse voltammetry (DPV) in the range of −1.1 to 1.1 V (Fig. 2). The four reversible processes at −0.78, −0.38, 0.42 and 0.85 V are ascribed to the stepwise one-electron iron-based redox couples $\mathbf{1}^{1+}$–$\mathbf{1}^{0}$, $\mathbf{1}^{2+}$–$\mathbf{1}^{1+}$, $\mathbf{1}^{3+}$–$\mathbf{1}^{2+}$ and $\mathbf{1}^{4+}$–$\mathbf{1}^{3+}$, respectively. The comproportionation constants K_c for $\mathbf{1}^{1+}$, $\mathbf{1}^{2+}$ and $\mathbf{1}^{3+}$ species are calculated as 4.07×10^6, 3.63×10^{13} and 1.95×10^7, respectively.

$$\underset{\mathbf{1}^{0}}{[Fe^{II}_4L_4]^0} \xrightarrow{E_1} \underset{\mathbf{1}^{1+}}{[Fe^{II}_3Fe^{III}L_4]^+} \xrightarrow{E_2} \underset{\mathbf{1}^{2+}}{[Fe^{II}_2Fe^{III}_2L_4]^{2+}} \xrightarrow{E_3} [Fe^{II}Fe^{III}_3L_4]^{3+} \xrightarrow{E_4} [Fe^{III}_4L_4]^{4+}$$

$$[Fe^{II}_4L_4]^0 + [Fe^{II}_2Fe^{III}_2L_4]^{2+} \overset{K_{c1}}{\rightleftharpoons} [Fe^{II}_3Fe^{III}L_4]^+ \quad (1)$$

$$[Fe^{II}Fe^{III}_3L_4]^{3+} + [Fe^{II}_3Fe^{III}L_4]^+ \overset{K_{c2}}{\rightleftharpoons} [Fe^{II}_2Fe^{III}_2L_4]^{2+} \quad (2)$$

$$[Fe^{III}_4L_4]^{4+} + [Fe^{II}_2Fe^{III}_2L_4]^{2+} \overset{K_{c3}}{\rightleftharpoons} [Fe^{II}Fe^{III}_3L_4]^{3+} \quad (3)$$

These values are larger than or comparable with the values of the Creutz–Taube salts,[11] revealing the pronounced thermodynamic stability of these mixed-valence species, especially, the di-mixed-valence complex $\mathbf{1}^{2+}$ in solution. Due in part to the extensive electronic delocalization and the sufficient interaction between the redox centers, the di-mixed-valence compound $\mathbf{1}^{2+}$ as well as $\mathbf{1}^{1+}$ and $\mathbf{1}^{3+}$ are likely to be isolated as pure samples.[10]

Variable-temperature magnetic susceptibility data for polycrystalline powder of compound $\mathbf{1}^{2+}$ identified by XRD as a pure phase were acquired for investigating the ground state electronic structure of $\mathbf{1}^{2+}$ (supporting information,† Fig. S2). The value of $\chi_M T$ at room temperature of 1.86 emu K mol^{-1} is close to the value expected for two uncoupled $S = 1/2$ ions with a g-factor of 2.73, suggesting the presence of two low-spin Fe^{III} centers and two low-spin Fe^{II} centers in the square. Upon cooling from room temperature, the value of $\chi_M T$ showed a continuous decrease to 1.50 emu K mol^{-1} at 20 K and then decreases dramatically to a value of 1.04 emu K mol^{-1} at 2 K. The best non-linear curve fitting of the χ_M *vs.* T data through simple regarding of a two $S = \frac{1}{2}$ metal centers model gave a g-factor value of 2.73 and $J = -1.30$ cm^{-1}, indicating a weak antiferromagnetic interaction between two low-spin Fe^{III} centers (supporting information,† Fig. S2). Considering the weak antiferromagnetic coupling and the inherent Coulombic repulsion between ions, it is reasonable to say that the two low-spin Fe^{III} centers occupy the opposite corners of the square with two-fold degenerate states.[12] Despite that di-mixed-valence molecular squares with homovalent metal centers being arranged in the opposite dots have been reported by step-to-step preparation[13] or step-to-step[14] oxidization of the original molecules, the self-assembly of mixed-valence molecular squares with the self-arrangement of the electronic distribution is quite significant.

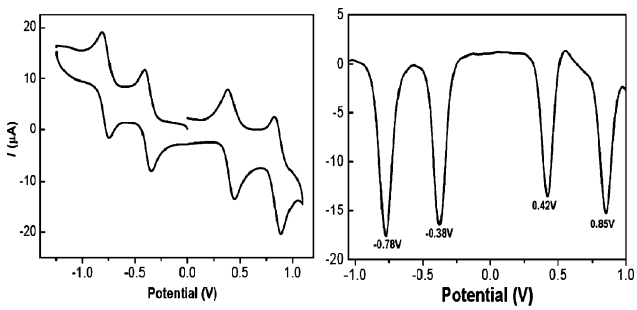

Fig. 2 CV (left) and DPV (right) of compound $\mathbf{1}^{2+}$ (1×10^{-3} M) in CH_3CN solution *vs.* Ag/AgCl couple at scan rates of 100 and 50 mV s^{-1}, respectively.

UV-Vis-NIR absorption spectrum of $\mathbf{1}(ClO_4)_2{\cdot}H_2O$ reveals an intense MLCT transition band centered at *ca.* 495 nm and a weak LMCT transition feature at *ca.* 825 nm (Fig. 3). In the near-IR range, the compound shows a band at about 1260 nm (7920 cm^{-1}) and a weak shoulder at about 1790 nm (5600 cm^{-1}). It can be safely attributed to intervalence charge transfer (IVCT) from the fully occupied t_2 orbitals of the Fe^{II} centers to the singly occupied t_2 orbitals of the Fe^{II} centers.[15] The small spin–orbit coupling of Fe^{III} ($\xi \approx$ 400–500 cm^{-1}) lead to closely spaced IT bands with overlapping absorptions as well as IC bands being shifted into the IR range with greatly reduced absorptivity.[16] Thus the splitting of the IT band of compound $\mathbf{1}^{2+}$ might contribute to the degeneracy of the excited states in such a tetranuclear square.

The IVCT band is nearly solvent independent (in DMF, CH_2Cl_2 and CH_3CN solvents) and solvent reorganization associated with the electron transition for $\mathbf{1}^{2+}$ is small, showing a considerable electron delocalization in the system.[16] The relationship of the ν_{max} of the IVCT band with the polarity of the solvent is also helpful in classifying the mixed-valence compounds. The plot gives a straight line with an intercept of *ca.* 7800 cm^{-1} (supporting information,† Fig. S3), which is interpreted as the Franck–Condon inner sphere optical activation energy. The narrow bandwidth (2500 cm^{-1}) at the half-maximum ($\Delta\nu_{1/2}$) of this IT band (compared with the value

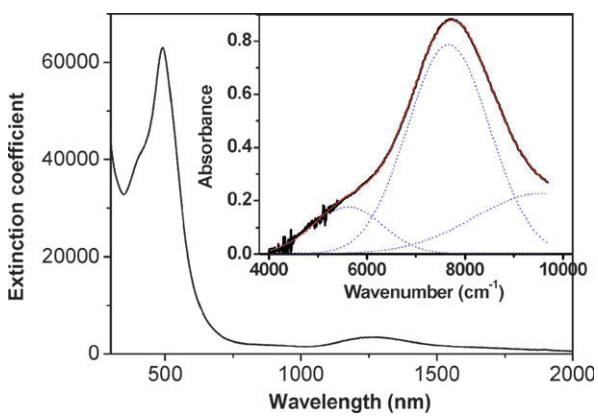

Fig. 3 UV-Vis-NIR spectrum of $\mathbf{1}^{2+}$ (1×10^{-4} M) in CD_3CN with the inset showing the IVCT band against wavenumber.

This journal is © The Royal Society of Chemistry 2008

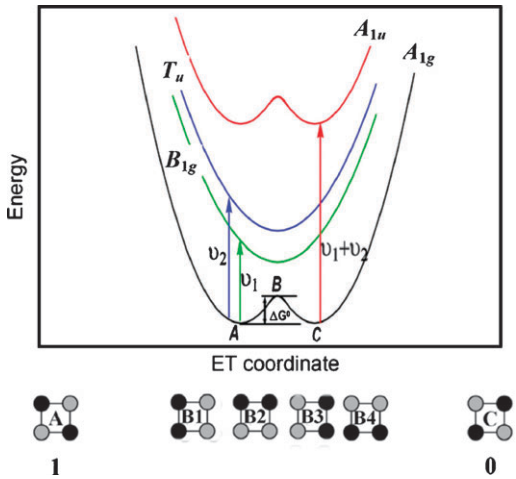

Fig. 4 Schematic two-well potential illustrating the tunable barriers induced by the presence of the intermediate states (B) with two excess electrons sited in one edge of the molecular square. The black balls represent the Fe^{II} centers, while the gray balls show the Fe^{III} centers.

(4200 cm^{-1}) derived from the equation $\nu_{max} = (\Delta\nu_{1/2})^2/2310$ at high-temperature limit) casts complex $\mathbf{1}^{2+}$ as a delocalized system. By applying a multi-dimensional electron transfer theory developed by Lambert,[17] we attempt to explain the splitting of the IT bands. The six diabatic states of $\mathbf{1}^{2+}$ (labeled by A, B and C) are shown at the bottom of Fig. 4. While the four B diabatic states have the same energy level, the other two diabatic states (A and C) are at lower energy level due to electrostatic repulsion. The meta coupling V_2 between the B diabatic states is set to be zero because it is expected to be much smaller than V owing to the meta conjugation path. Having performed these simplifications, the secular determinant, in which only the diabatic states A(C) couple with B states, is shown in eqn (4).

$$\begin{vmatrix} \lambda_A\text{-}\varepsilon\text{-}\Delta G^\circ & V & V & V & V & 0 \\ V & \lambda_{B1}\text{-}\varepsilon & 0 & 0 & 0 & V \\ V & 0 & \lambda_{B2}\text{-}\varepsilon & 0 & 0 & V \\ V & 0 & 0 & \lambda_{B3}\text{-}\varepsilon & 0 & V \\ V & 0 & 0 & 0 & \lambda_{B4}\text{-}\varepsilon & V \\ 0 & V & V & V & V & \lambda_C\text{-}\varepsilon\text{-}\Delta G^\circ \end{vmatrix} = 0 \quad (4)$$

Here ΔG° is the net energy difference between the potentials of states with the two Fe^{III} at diagonal positions and that at *ortho* positions, which mainly arises from the electrostatic repulsion potential and potential magnetic interactions; λ is the diabatic potential corresponding to each diabatic states.

Diagonalisation of the matrix in the eqn (4) yields the adiabatic ground state (A_{1g} in the delocalized D_{4h} case) and excited states (T_u, B_{1g}, A_{1u}). In case of the valence delocalized complex $\mathbf{1}^{2+}$, the energy difference between the lower energy IVCT (ν_1) and the higher energy IVCT (ν_2) should be equal to the energy difference ΔG° (2320 cm^{-1}), whereas the electron coupling potential V is determined by using $(\nu_1\nu_2/8)^{\frac{1}{2}}$ as 2350 cm^{-1}. The thermal free energy barrier ΔG^* ($\sim 10k_BT$) that electronic transfer needs to overcome by a thermal pathway within the ground states should be larger than the energy difference ΔG°. This value allows $\mathbf{1}^{2+}$ to maintain its stable binary states with rare thermodynamic mistakes and switch when induced at room temperature in the QCA application. In summary, the thermally induced consecutive single electron transfers in the ground states *via* one of these intermediates (the true saddle points) (A → B → C) are preferred over alternative concerted two-electron transfer directly occurs between the ground states A and C, since the electrons can only populate the space around the edges of the square. This two-step mechanism might benefit device clocking, which not only permits control of information flow around the circuit but also enables true power gain relevant to power dissipation in QCA devices.[18]

This work is supported by the National Natural Science Foundation of China (20571041) and the Start-Up Fund of Dalian University of Technology.

Notes and references

‡ *Crystal data* for compound $\mathbf{1}\cdot(ClO_4)_2\cdot H_2O$, $C_{100}H_{74}Cl_2Fe_4N_{24}O_9S_4$, M_r = 2196.39, orthorhombic, space group *Pbcn*, a = 14.294(1), b = 24.050(2), c = 28.334(2) Å, V = 9740.1(13) Å^3, μ = 0.797 mm^{-1}, Z = 4, T = 293 K. 51 865 reflections were collected of which 8578 reflections were unique (R_{int} = 0.0812). The final refinement gave R_1 = 0.0709 and wR_2 = 0.2143 for 6426 reflections with $I \geq 2\sigma(I)$.

1 J. M Lehn, *Science*, 2002, **295**, 2400; C. Joachim, J. K. Gimzewski and A. Aviram, *Nature*, 2000, **408**, 541.
2 Z. Zhong, D. Wang, Y. Cui, M. W. Bockrath and C. M. Lieber, *Science*, 2003, **302**, 1377; M. Ruben, J. Rojo, F. J. Romero-Salguero, L. H. Uppadine and J. M. Lehn, *Angew. Chem., Int. Ed.*, 2004, **43**, 3644.
3 P. J. Low, *Dalton Trans.*, 2005, 2821; A. O. Orlov, I. Amlani, G. H. Bernstein, C. S. Lent and G. L. Snider, *Science*, 1997, **277**, 928; I. Amlani, A. O. Orlov, G. Toth, G. H. Bernstein, C. S. Lent and G. L. Snider, *Science*, 1999, **284**, 289.
4 A. Imre, G. Csaba, L. Ji, A. O. Orlov, G. H. Bernstein and W. Porod, *Science*, 2006, **311**, 205.
5 J. Jiao, G. J. Long, L. Rebbouh, F. Grandjean, A. M. Beatty and T. P. Fehlner, *J. Am. Chem. Soc.*, 2005, **127**, 17819; C. S. Lent, *Science*, 2000, **288**, 1597.
6 C. S. Lent, B. Isaksen and M. Lieberman, *J. Am. Chem. Soc.*, 2003, **125**, 1056; H. Qi, S. Sharma, Z. Li, G. L. Snider, A. O. Orlov, C. S. Lent and T. P. Fehlner, *J. Am. Chem. Soc.*, 2003, **125**, 15250.
7 F. A. Cotton, C. Lin and C. A. Murillo, *J. Am. Chem. Soc.*, 2001, **123**, 2670; V. C. Lau, L. A. Berben and J. R. Long, *J. Am. Chem. Soc.*, 2002, **124**, 9042; H. Yao, M. Sabat, R. N. Grimes, F. Fabrizi de Biani and P. Zanello, *Angew. Chem., Int. Ed.*, 2003, **42**, 1002; F. A. Cotton, C. Y. Liu, C. A. Murillo and X. Wang, *Chem. Commun.*, 2003, 2190.
8 P. J. Stang and B. Olenyuk, *Acc. Chem. Res.*, 1997, **30**, 502; S. Leininger, B. Olenyuk and P. J. Stang, *Chem. Rev.*, 2000, **100**, 853.
9 C. He, C. Y. Duan, C. J. Fang, Y. J. Liu and Q. J. Meng, *J. Chem. Soc., Dalton Trans.*, 2000, 1207.
10 R. R. Gagné, C. L. Spiro, T. J. Smith, C. A. Hamann, W. R. Thies and A. K. Shiemke, *J. Am. Chem. Soc.*, 1981, **103**, 4073; R. Lomoth, A. Magnuson, Y. Xu and L. Sun, *J. Phys. Chem. A*, 2003, **107**, 4373.
11 C. Creutz, *Prog. Inorg. Chem.*, 1983, **30**, 1; C. Creutz and H. Taube, *J. Am. Chem. Soc.*, 1973, **95**, 1086.
12 S. J. Yoo, Z. Hu, C. Goh, E. L. Bominaar, R. H. Holm and E. Münck, *J. Am. Chem. Soc.*, 1997, **119**, 8732.
13 L. H. Uppadine and J. M. Lehn, *Angew. Chem., Int. Ed.*, 2004, **43**, 240.
14 J. Jiao, G. J. Long, F. Grandjean, A. M. Beatty and T. P. Fehlner, *J. Am. Chem. Soc.*, 2003, **125**, 7522.
15 D. M. D'Alessandro and F. R. Keene, *Chem. Rev.*, 2006, **106**, 2270; M. Fabre and J. Bonvoisin, *J. Am. Chem. Soc.*, 2007, **129**, 1434.
16 K. D. Demadis, C. M. Hartshorn and T. J. Meyer, *Chem. Rev.*, 2001, **101**, 2655.
17 C. Lambert, *ChemPhysChem*, 2003, **4**, 877.
18 J. Timler and C. S. Lent, *J. Appl. Phys.*, 2002, **91**, 823.